11th ANKARA INTERNATIONAL AEROSPACE CONFERENCE **AIAC-2021-068**
8-10 September 2021 - METU, Ankara TURKEY

NON-REACTING AND REACTING ANALYSIS OF VOLVO FLAME HOLDER USING LESTR3D AND OPENFOAM FLOW SOLVERS

Omer Yalili*, Mustafa Sengul†, Tamer Sener‡, and Ayse G. Gungor§
Faculty of Aeronautics and Astronautics, Istanbul Technical University, Istanbul, Turkey

ABSTRACT

The capabilities of an in-house flow solver lestr3d are presented in this study by simulating Volvo bluff body problem, and the effect of combustion on turbulence is investigated by comparing the flow features of reactive and non-reactive results. Volvo bluff body problem includes complex, 3D unsteady flow features and wall-vortex interactions; therefore, it is a good problem to present the capabilities of the in-house code. The problem is simulated using large eddy simulation for all cases, and for cold case, lestr3d flow solver is used with Smagorinsky and k-equation subgrid models, and OpenFOAM is used only with Smagorinsky model using the same mesh and boundary conditions. For the hot flow case, OpenFOAM flow solver is used with the same mesh with the cold flow case, and the reaction is modelled with partially stirred reaction (PaSR) combustion model. Results of lestr3d are in good agreement with OpenFOAM and experimental data for Volvo bluff body case. Cold flow results of lestr3d are compared with hot flow results of OpenFOAM to investigate the effect of combustion on turbulent flow. It was observed that, flame supresses the instabilities by introducing additional torque to the flow and broaden the recirculation zone. For the hot flow case the Karman street behind the bluff body is not observed and the interaction of bluff body generated vortexes and channel walls is broken.

INTRODUCTION

In the aerospace industry, bluff-body stabilized flames take an important part and this topic has been investigated for several decades. A detailed experimental study for premixed combustion to provide an understanding of bluff body stabilized flames and benchmark results for numerical models is conducted in Sjunnesson et al [1992]. To solve turbulent reactive flows, large eddy simulation (LES) can be considered as a promising method and has been widely employed by several researchers to simulate reactive flow in Volvo bluff body problem [Porumbel and Menon, 2006; Fureby, 2019; Verma et al, 2019]. In LES, large scales of the flow are resolved, and since small scales have isotropy, modelling small scales introduces less error to the simulation. Choosing combustion model and reaction mechanism is an important task while modelling combustion, and those should be done specific to thhe problem in hand. [Dryer and Westbrook, 1981] provided simplified one and two-

*Bs.C. Student in Aero. and Astro. Eng, Email: yalili@itu.edu.tr
†Ph.D. Student in Aero. and Astro. Eng, Email: sengulmu@itu.edu.tr
‡Ph.D. Student in Aero. and Astro. Eng., Email: senerta@itu.edu.tr
§Assoc. Prof, Email: ayse.gungor@itu.edu.tr

step reaction mechanisms for hydrocarbons. Also, [Fureby, 2018] compared the effect of reaction mechanism on accuracy by considering 2 to 766 step reactions, and several reaction models using bluff body problem.

In this study an in-house code, $lestr3d$, is used to simulate Volvo bluff body problem with LES. Results are compared with an open source code OpenFOAM results obtained with the same mesh and boundary conditions and experimental data to examine its compatibility. Besides, $lestr3d$ cold flow results are compared with the OpenFOAM reactive flow results to investigate the effect of combustion on coherent structures, vorticity and velocity fields. Results obtained with $lestr3d$ includes Smagorinsky and K-equaiton sub-grid-scale models while with OpenFOAM only Smagorinsky model is used. To model the reaction with OpenFOAM, partially stirred reaction (PaSR) combustion model with one-step global reaction is used.

Firstly, the governing equations for compressible LES and the PaSR combustion model are presented. Secondly, details of the $lestr3d$ solver are summarized. Lastly, the Volvo problem is introduced, flow structures and statistics of the cold and hot flows are presented and compared.

GOVERNING EQUATIONS

To obtain LES equations, a spatial filter should be applied to the Navier-Stokes (NS) equations since by methodology LES resolves main flow and models small scales, thus applying this filter separates those two. Filtering operation on any variable Ψ provides sum of large scale (solved by LES) component, $\overline{\Phi}$, and small scale (sgs) component Φ'; i.e $\Psi = \overline{\Phi} + \Phi'$. This separation between small and large scales is determined by a filter width size, $\overline{\Delta}$, and in this study box filter is employed by assuming that filter commutes with differentiation.

By giving a Favre-filtered quantity, Ψ, in the flow field as $\tilde{\Psi} = \overline{\rho\Psi}/\overline{\rho}$, governing equations of reactive LES for continuity, momentum, total energy, and species transport can be given, respectively as;

$$\frac{\partial \overline{\rho}}{\partial t} + \frac{\partial \overline{\rho}\tilde{u}_i}{\partial x_i} = 0; \tag{1}$$

$$\frac{\partial \overline{\rho}\tilde{u}_i}{\partial t} + \frac{\partial}{\partial x_j}[\overline{\rho}\tilde{u}_i\tilde{u}_j + \overline{p}\delta_{ij} - \tilde{\tau}_{ij} + \tau_{ij}^{sgs}] = 0; \tag{2}$$

$$\frac{\partial \overline{\rho}\tilde{E}}{\partial t} + \frac{\partial}{\partial x_i}[(\overline{\rho}\tilde{E} + \overline{p})\tilde{u}_i + \tilde{q}_i - \tilde{u}_j\tilde{\tau}_{ij} + H_i^{sgs}] = 0; \tag{3}$$

$$\frac{\partial \overline{\rho}\widetilde{Y_m}}{\partial t} + \frac{\partial}{\partial x_i}\left[\overline{\rho}\widetilde{u_i}\widetilde{Y_m} + \overline{\rho}\bar{V}_{i,m}\widetilde{Y_m} + \Phi_{i,m}^{sgs} + \theta_{i,m}^{sgs}\right] = \bar{\dot{w}}_m, \quad m = 1, N. \tag{4}$$

In these equations, i and j indices are used according to Einstein's summation convention, and they can be given as: $i = 1, 2, 3$ and $j = 1, 2, 3$. Here, t is time, x_i (or x_j) is spatial coordinates, $\tilde{u}_i$ (or $\tilde{u}_j$) is velocity, $\overline{p}$ is pressure, $\tilde{\tau}_{ij}$ and τ_{ij}^{sgs} are stress tensors in main flow and sgs, $\tilde{E}$ is energy, $\tilde{q}_i$ is heat flux, and H_i^{sgs} is sgs enthalpy flux. The last equation is species transport equation and here Y_m is mass fraction of m^{th} species, $\bar{V}_{i,m}$ is diffusion velocity in i^{th} direction, $\Phi_{i,m}^{sgs}$ is sgs convective mass flux, $\theta_{i,m}^{sgs}$ is sgs diffusive mass flux, and $\bar{w}_m$ is reaction rate of m^{th} species.

Sgs terms, τ_{ij}^{sgs}, H_i^{sgs}, and ϕ_{im}^{sgs}, in LES equations need to be modelled. It should be noted that in species transport equation sgs diffusive mass flux θ_{im}^{sgs} is neglected, because there is no conventional closure for that term [Poinsot and Veynante , 2012]. Compressible version [Erlebacher et al, 1992] of Smagorinsky model [Smagorinsky, 1963] and k-equation model is used to compute sgs stress tensor, τ_{ij}^{sgs}.

Lastly, sgs enthalpy flux is calculated using the eddy viscosity approach $H_i^{sgs} = -\frac{\bar{\rho}\nu_T}{Pr_t}\frac{\partial \tilde{H}}{\partial x_k}$, noting that the total enthalpy per unit mass is $\tilde{H} = \tilde{E} + \overline{p}/\overline{\rho}$, H_i^{sgs}. For the sake of simplicity, turbulent Prandtl number, Pr_t, is set to unity.

Combustion Modeling

The PaSR model is a detailed chemistry model and stands on the assumption that the computational cell is divided into two fraction zones which are reacting and nonreacting. The reacting zone acts as a perfectly stirred reactor, in which whole species are perfectly stirred and reacted with each other. Then, the new calculated species from reacting part blends whole domain owing to turbulent effects by mixing time τ_{mix} Li et al. [2018]. According to the PaSR reaction model, the mass fraction of reactive region is calculated as

$$\kappa = \frac{\tau_c}{\tau_c + \tau_{mix}} \tag{5}$$

where, τ_c is characteristic time of chemical reaction and τ_{mix} represents characteristic mixing time. The mean reacting rate of cell $\overline{\dot{w}_i}$ is calculated by creating a concentration exchange relationship between two zones by

$$\overline{\dot{\omega}_k} = \kappa \frac{\overline{\rho}(Y_i^* - Y_i^0)}{\tau^*} = \kappa \dot{\omega}_k. \tag{6}$$

Here, Y_i^* denotes mass fractions of species in reacting zone, Y_i^0 presents mass fraction of species in non-reacting zone and τ^* is characteristic residence time.

Even though the detailed and skeletal chemistry mechanisms provide highly accurate and comprehensive results, they require excessive computational cost. On the other hand, the global mechanisms are able to simulate the turbulent reacting flow features properly without extensive cost. Owing to its simplicity and accuracy, the mechanism of propane reaction is modelled with one global step as [Dryer and Westbrook, 1981]:

$$C_3H_8 + 5O_2 + \frac{395}{21}N_2 \rightarrow 3CO_2 + 4H_2O + \frac{395}{21}N_2. \tag{7}$$

The Arrhenius law is used for the calculation of the reaction rate, and it is defined as

$$k = AT^b e^{-\frac{E_a}{R\,T}} C_{C_3H_8}^{0.1} C_{O_2}^{1.65}. \tag{8}$$

Here, E_a represents the energy of activation that is $3 \times 10^4\ \frac{cal}{g}$, R is the universal gas constant, A and b are experimental constants which are 8.6×10^{11} and 1.65, respectively.

VOLVO BLUFF BODY PROBLEM

Volvo bluff body problem has a rectangular cross-section and an equilateral triangular bluff body located at the centerline of the channel. In Figure 1 the geometry of the problem is depicted next to the mesh used during the simulations. The dimension D in Figure 1 is equal to $0.04m$ which is also the bluff body edge. The computational domain is discretized into 5 million structured mesh elements using 20 blocks for both hot and cold flow simulations. Meshes near the bluff body wake and walls are refined to capture the high shear behavior of the flow near those regions. The boundary conditions of this study can be summarized as: no slip conditions at walls and prism surfaces, periodic boundary conditions at front and back faces, bulk velocity at inlet and zero gradient at outlet.

The detailed operating conditions that are used in simulations in this study, for non-reactive and reactive cases, are presented in Table 1.

RESULTS

The cold flow results presented here are obtained with our in-house $lestr3d$ program using Smagorinsky (this combination will be mentioned as $lestr3d$-Smag) and k-equation (this combination will be mentioned as $lestr3d$-Keq) models. $lestr3d$ is a cartesian coordinate solver for subsonic compressible gas flow. This code is written in FORTRAN using the cell-centered finite volume method for unstructured grids and parallelized with message passing interface. To apply boundary conditions ghost cell methodology is used. The details of our in-house flow solver are given in [Karahan, 2017; Er,

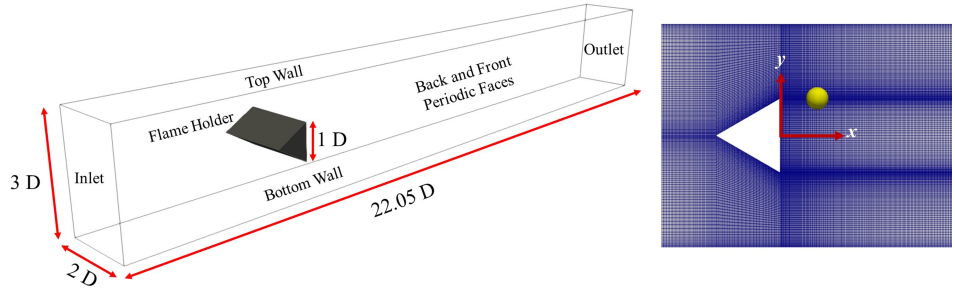

Figure 1: Problem geometry and generated mesh near bluff body.

Table 1: Operating conditions Sjunnesson et al [1992].

Operating conditions	Non-Reactive Case (Cold)	Reactive Case (Hot)
Bulk velocity	16.6 m/s	17.3 m/s,
Bulk Reynolds number	45578	47000
Inlet temperature	-	288 K
Mass flow rate	0.1994	0.2079
Premixed Fuel/Oxidizer	-	Propane/Air
Equivalence ratio	-	0.62

2019]. OpenFOAM simulations are conducted using Smagorinsky model with pisoFOAM solver for cold flow, and PaSR model with reactingFOAM solver for hot flow. The second order discretization scheme is used for spatial discretization on an unstructured mesh for both programs. For the temporal disretization, first order Euler method is used with OpenFOAM solver while 2 stage Runge-Kutta scheme is used for *lestr3d*. Timestep is determined adaptively for both solvers using CFL numbers which is 1 for *lestr3d*, 0.6 for non-reacting OpenFOAM and 0.4 for reacting OpenFOAM simulations. The statistics are collected with OpenFOAM for 20 FTT, 17 FTT with *lestr3d*-Smag and 5 FTT *lestr3d*-Keq. In this part, cold flow results of *lestr3d* flow solver is compared with OpenFOAM using same geometry, mesh and boundary conditions. Also, to examine the effect of combustion on flow, cold flow results are compared with reactive flow results of OpenFOAM.

Mesh resolution

To check the accuracy of the results in this work, a probe data is collected during the simulations. The probe is located on $x/D = 0.5$, $y/D = 0.5$ and $z/D = 1$, and can be seen in Figure 1 as a point on mesh. The shedding frequency, and corresponding Strouhal number, $St = \frac{fL}{U}$, is given in Table 2. This table shows that the obtained shedding frequencies and St numbers are in harmony with the data in the literature.

Table 2: Vortex shedding frequencies.

	Vortex Shedding Frequency		St number	
	Cold	Hot	Cold	Hot
Present - OpenFOAM	120	126	0.25	0.2913
Present - *lestr3d*-Smag	124.87	-	0.30	-
Present - *lestr3d*-Keq	125	-	0.30	-
Literature	105 Sjunnesson et al [1992]	140 Porumbel [2006]	0.25 Sjunnesson et al [1992]	0.3236 Porumbel [2006]

Reaction effect on flow and statistics

Figure 2 depicts the coherent structures obtained with Q criterion and z-vorticity field at the mid plane for cold and hot flows. The results are obtained with *lestr3d*-Smag for cold and OpenFOAM for hot flows are investigated. Figure 2 shows that, for the cold flow there is an acute interaction between the upper and lower walls and the bluff body generated turbulence. The bluff body creates

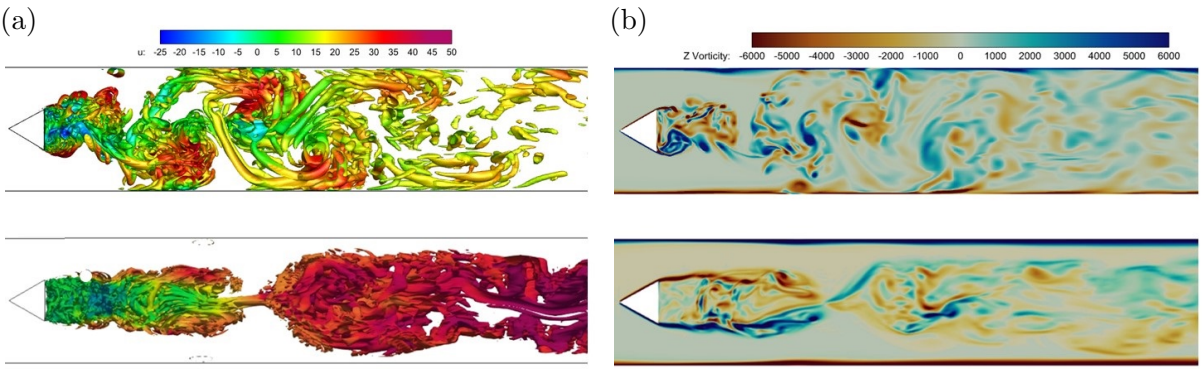

Figure 2: Instantaneous second invariant of the velocity gradient tensor, Q colored by axial velocity (a), and z-vorticity at the mid plane (b). Top: cold *lestr3d*-Smag, bottom: hot OpenFOAM.

a recirculation zone that extends an edge length at the aft of it, and at some point the shear layer at the trailing edge brokes down which causes to Kelvin-Helmholtz instabilities to occur. Moving downstream, the intensity of the turbulance decays and flow recovers. The reaction altered the flow behavior that can be observed from the hot flow results. The recirculation zone expands and the Kelvin-Helmholtz instabilities are suppressed. Also, the flow behind the bluff body becomes symmetric and the vortexes shrinked due the reaction.

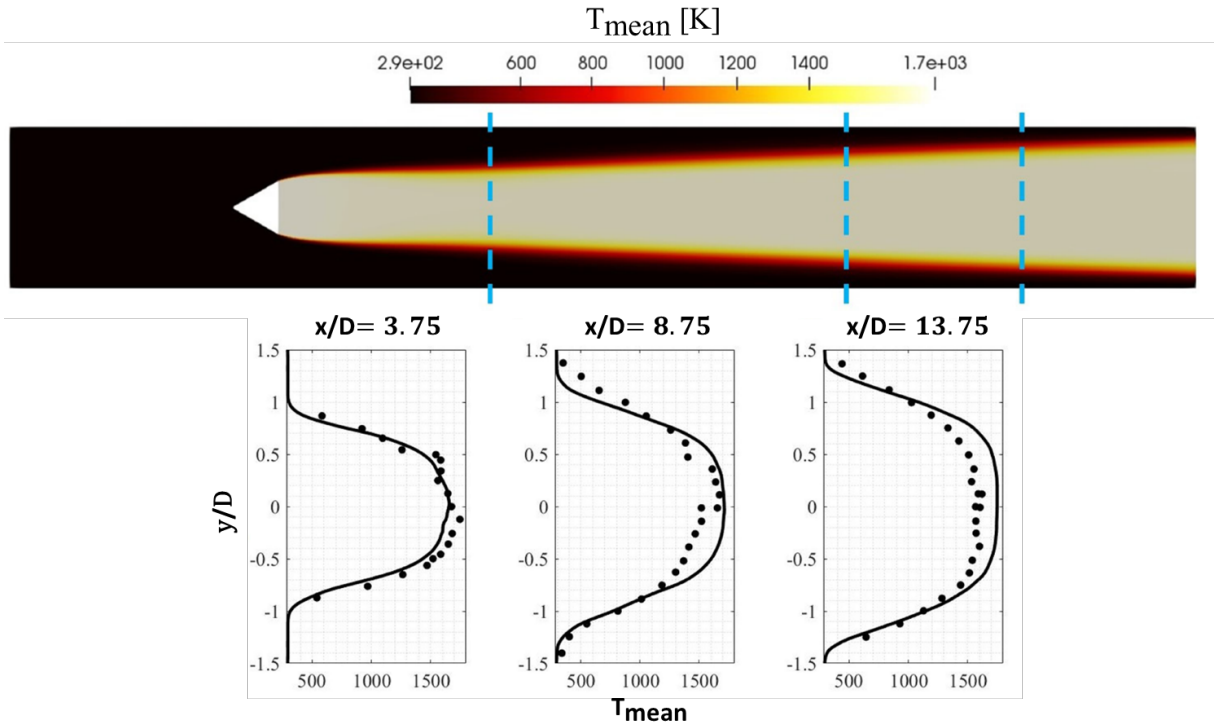

Figure 3: Mean temperature field and the transverse distribution of temperature at three stations.

The hot flow result for temperature obtained with OpenFOAM is given in Figure 3. The flame is stabilized by the shear layer behind the bluff body. The recirculation zone, shown in Figure 2 mixes the burned and unbuurned fresh gases and sustains the reaction. The heat released from the burned gases ignites the fresh gases and therefore the reaction continues. The flame observed to expand near the outlet.

The statistics of cold and hot flows are collected for cold and hot cases and compared with experimental data. The cold flow results of *lestr3d*-Smag, *lestr3d*-Keq are compared with each other, and OpenFOAM in terms of performance with this problem. The results are presented at five lo-

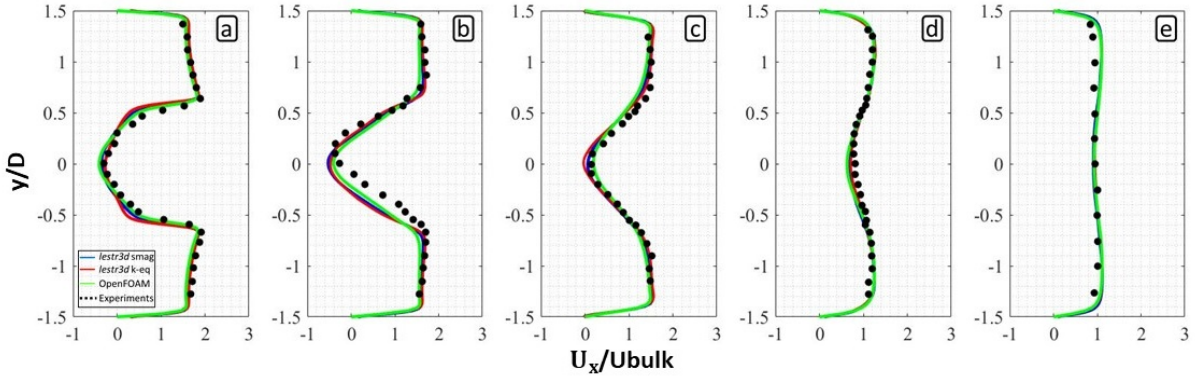

Figure 4: Cold flow. Normalized axial mean velocity distributions behind the bluff body. Station locations: (a) $x/D = 0.375$, (b) $x/D = 0.95$, (c) $x/D = 1.53$, (d) $x/D = 3.75$, (e) $x/D = 9.4$.

cations measured from bluff body, and those locations named as a,b,c,d,e of which locations are $x/D = 0.375, 0.95, 1.53, 3.75, 9.4$, respectively. Mean velocity distribution in transversal direction is presented in Figure 4. *lestr3d*-Smag and *lestr3d*-Keq show similar behavior through the channel and those results are in harmony with the experimental data and OpenFOAM cold flow results. In particular *lestr3d*-Smag results coincide with OpenFOAM results which is also simulated with Smagorinsky model. It can be concluded that, *lestr3d*'s numerical scheme and integration scheme are in coherence with OpenFOAM. Overall, the axial mean velocity shows symmetrical behavior within the channel. The strong wake dominates the flow in the first three stations, and moving downstream the wake loses its effect and the flow becomes almost uniform. The flow is accelerated on the top and the bottom of the bluff body because of reduction in the flow area.

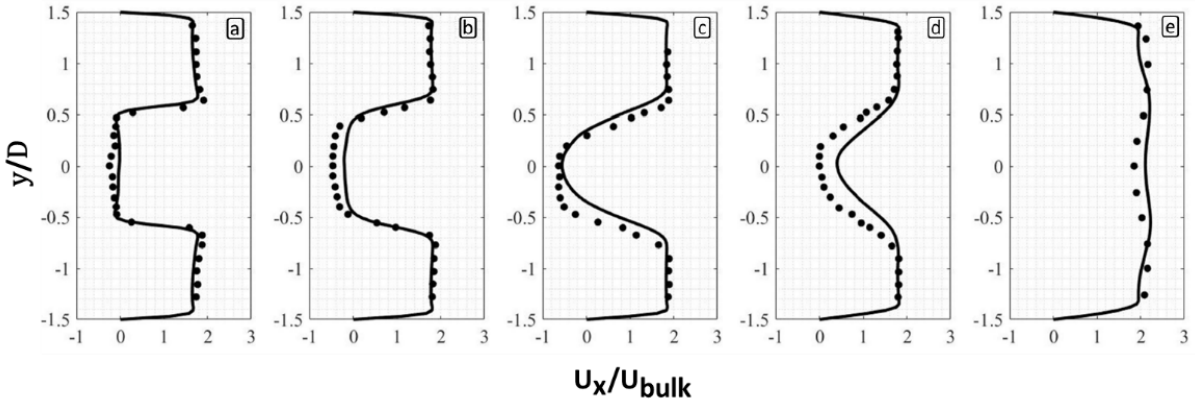

Figure 5: Reacting flow. Normalized axial mean velocity distributions behind the bluff body.

Figure 5 visualizes the mean axial velocity for the reacting case obtained with OpenFOAM. The velocity just behind the bluff body or the flame core is approximately zero. The velocity of the unburned mixture drops significantly at the reaction zone. Because the heat released from the reaction causes the fluid to expand, the flow is accelerated at the outlet. The recirculation zone is expanded to the fourt station compared to cold flow.

Axial velocity rms values for *lestr3d*-Smag and *lestr3d*-Keq are given with Figure 6. Plots of both models are matches well with the experimental data, and both sgs models shows similar behavior.

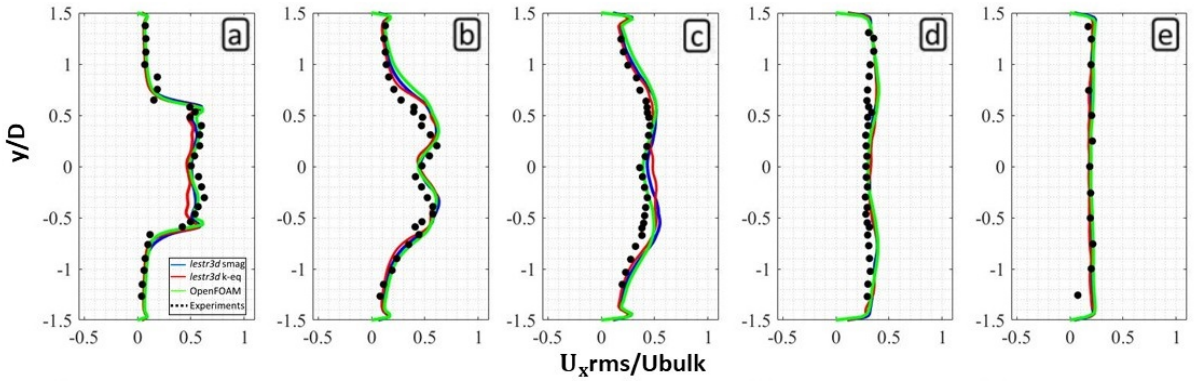

Figure 6: Cold flow. Normalized axial rms velocity distributions behind the bluff body.

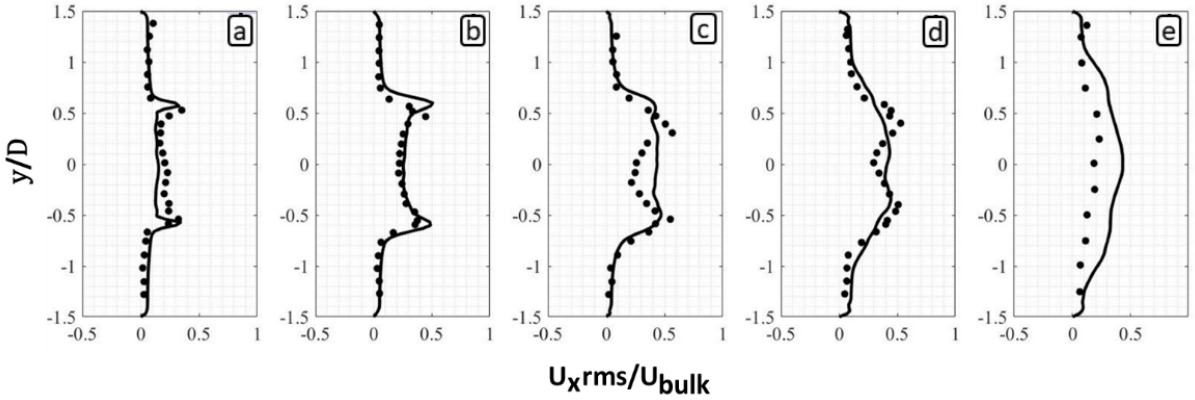

Figure 7: Reacting flow. Normalized axial rms velocity distributions behind the bluff body.

Also the results for both sgs models are in agreement with OpenFOAM results. At station (a), the shear layer is strong at bluff body trailing edges, and there are two peaks in rms velocity. This peaks drops at station (b) and are not observed at station (c) where the shear layer cannot be observed as a single layer.

In Figure 7 rms velocities in axial direction are presented for each station. First two stations are predicted well with OpenFOAM, and last three stations OpenFOAM captures the trend of the experimental results. The shear layer acts strongly in at the two trailing corners of the bluff body, and this effect is seen as two peaks in the graps. These peak rms velocities does not decreases until fourth station, thus the shear layer, where flame holds, lies until approximately $x/D = 3.75$. Those two peaks are also observed in the cold flow, but the reaction increases the stress and therefore the rms velocities near the trailing corners are intensified.

CONCLUSION

Cold flow results of Volvo bluff body problem is presented using an in-house, second order finite volume based flow solver, *lestr3d* using Smagoringsky and k-equation subgrid models, and open-source flow solver OpenFOAM using Smagorinsky model. Hot flow results are obtained using the same mesh and geometry using OpenFOAM with PaSR combustion model and one-step global reaction.

Cold flow results obtained with *lestr3d* are compared with an open source flow solver OpenFOAM and experimental data. *lestr3d* results show good agreement with OpenFOAM and experimental data, indicating the capabilities of the in house solver *lestr3d* for complex turbulent flows. The flow behind the bluff body is well captured with both subgrid models.

Combustion effect on flow for the same problem is investigated by simulating reaction by OpenFOAM. In general, combustion widens the recirculation zone and accelerates the flow within the channel. Besides, the Kelvin-Helmholtz instabilities seen in the non-reactive simulations are suppressed with the flame, therefore Karman street behind the bluff body is not observed. On the trailing edges of the bluff body the rms velocities are intensified with the combustion, which means shear layer becomes stronger on the aft of the bluff body.

We will enhance our in-house solvers capabilities by adding combustion featiure and examine the effects of pressure gradient and combustion model effect on the flow and flame.

ACKNOWLEDGEMENTS

This work is funded by the Scientific and Technological Research Council of Turkey (TUBITAK) under grant number 219M139.

References

Cocks, P., A., T., Soteriou M., C., Sankaran, V.(2015) *Impact of numerics on the predictive capabilities of reacting flow LES*, Combustion and Flame, Vol 162, p:3394-3411, 2015.

Dryer, F. L., Westbrook, C., K.(1981) *Simplified Reaction Mechanisms for the Oxidation of Hydrocarbon Fuels in Flames*, Combustion Science and Technology, 1981.

Er, S.(2019) *A finite volume based in-house large eddy simulation solver for turbulent flows in complex geometries*, Master's Thesis, Istanbul Technical University Department of Aeronautics and Astronautics Engineering.

Erlebacher, G, Hussaini, M. Y., Speziale, C. G. and Zang, T. A.(1992) *Toward the large-eddy simulation of compressible turbulent flows* J. Fluid Mech., Vol 238, p: 155-185.

Fureby, C.(2018) *The volvo validation rig – A comparative study of large eddy simulation combustion models at different operating conditions*, AIAA Aerospace Sciences Meeting, Jan 2018.

Fureby, C.(2019) *A large eddy simulation (LES) study of the VOLVO and AFRL bluff body combustors at different operating conditions*, AIAA Scitech Forum, Jan 2019.

Fureby, C. and Möller, S. I.(1995) *Large eddy simulation of reacting flows applied to bluff body stabilized flames*, AIAA Journal, Vol 33, p:2339-2347, 1995.

Karahan,D., T.(2017) *A new large eddy simulation solver for wall-bounded turbulent flows*, Master's Thesis, Istanbul Technical University Department of Aeronautics and Astronautics Engineering.

Karahan, D. T., Er, S., Gungor, A. G.(2017) *Large Eddy Simulation of Wall-Bounded Turbulent Flows*, Ankara International Aerospace Conference, Sep 2017.

Li, Z., Ferrarotti, M., Cuoci, A., Parente, A. (2018) *Finiterate chemistry modelling of non-conventional combustion regimes using a Partially-Stirred Reactor closure: Combustion model formulation and implementation details*, Applied energy, Vol 225, p: 637-655.

Porumbel, I.(2006) *Large Eddy Simulation of bluff body stabilized premixed and partially premixed combustion*, Ph. D. Thesis, School of Aerospace Engineering Georgia Institute of Technology.

Porumbel, I., Menon, S.(2006) *Large Eddy Simulation of Bluff Body Stabilized Premixed Flames in Vitiated Crossflow*, 44th AIAA Aerospace Science Meeting and Exhibit, Jan 2006.

Sjunnesson, A. and Henrikson, P. and Löfström, C.(1992) *Cars measurements and visualization of reacting flows in a bluff body stabilized flame*, AIAA/ASME/SAE/ASEE 28th Joint Propulsion Conference and Exhibit, Jul 1992.

Smagorinsky, J.(1963) *General circulation experiments with the primitive equations I. The basic experiment*, Monthly Weather Review, Vol 91, No 3, p: 99-164.

Thierry, P. and Veynante, D. (2012) *Theoretical and Numerical Combustion*, RT Edwards, Inc.

Verma, I., Yadav, R., Orsino, S., Sharkey, P., Nakod, P.(2019) *Large eddy simulations of premixed bluff body stabilized flame using detailed chemistry with flamelet generated manifold: Grid sensitivity analysis*, AIAA Scitech Forum, Jan 2019.